U.S. Department
Of Transportation

People Saving People
http://www.nhtsa.dot.gov

Anthropometric Evaluation of THOR-05F

Sheila M. Ebert
Matthew P. Reed

University of Michigan Transportation Research Institute

April 2013

Technical Report Documentation Page

1. Report No.	2. Government Accession No.	3. Recipient's Catalog No.
UMTRI-2013-12		

4. Title and Subtitle	5. Report Date
Anthropometric Evaluation of THOR-05F	April 2013
	6. Performing Organization Code
7. Author(s) Ebert, Sheila M. and Reed, Matthew P.	8. Performing Organization Report No.
9. Performing Organization Name and Address University of Michigan Transportation Research Institute 2901 Baxter Rd. Ann Arbor MI 48109	10. Work Unit No. (TRAIS)
	11. Contract or Grant No.
12. Sponsoring Agency Name and Address National Highway Traffic Safety Administration	13. Type of Report and Period Covered
	14. Sponsoring Agency Code

15. Supplementary Notes

16. Abstract

An exemplar THOR-05F was compared to the anthropometric specification from the Anthropometry of Motor Vehicle Occupants (AMVO) study on a wide variety of dimensions, including segment lengths, masses and CG locations; relative joint and landmark positions; and external body contours. Overall, the ATD matched the specifications well. Four potentially significant discrepancies were noted:

1. The upper-arm segment of the THOR-05F is shorter than the AMVO specification.
2. The shoulder cannot readily be placed into the driving posture represented by the AMVO contour, which might affect the realism of seat belt fit in some circumstances.
3. The THOR-05F buttock contour differs substantially from the AMVO contour, but the differences may represent an appropriate compromise given the differences between ATD and human flesh.
4. The jacket components representing breast tissue may not have sufficient positional control, potentially affecting belt routing and thoracic response.

Based on these observations, five recommendations were made:

1. Consideration should be given to lengthening the upper arm segment by 35 mm to better match the AMVO specification.
2. The static positioning of the shoulder components should be examined to determine if a more realistic driving posture could be created.
3. The vertical position of the ATD as installed in vehicle seats should be compared to the positioning of similar-size occupants to address the buttock contour concerns.
4. The effects of the jacket and breast components on belt routing relative to the pelvis, thorax, and shoulder should be examined to determine if greater control of the installation and positioning of these soft components is needed to ensure test repeatability and reproducibility.
5. Future ATD development efforts should include the provision of physical landmarks on the ATD to support anthropometric verification.

17. Key Word	18. Distribution Statement
ATD, crash test dummy, THOR, anthropometry	

19. Security Classif. (of this report)	20. Security Classif. (of this page)	21. No. of Pages	22. Price
		47	

Form DOT F 1700.7 (8-72) Reproduction of completed page authorized

Metric Conversion Chart

APPROXIMATE CONVERSIONS TO SI UNITS

SYMBOL	WHEN YOU KNOW	MULTIPLY BY	TO FIND	SYMBOL
LENGTH				
In	inches	25.4	millimeters	mm
Ft	feet	0.305	meters	m
Yd	yards	0.914	meters	m
Mi	miles	1.61	kilometers	km
AREA				
in^2	squareinches	645.2	square millimeters	mm^2
ft^2	squarefeet	0.093	square meters	m^2
yd^2	square yard	0.836	square meters	m^2
Ac	acres	0.405	hectares	ha
mi^2	square miles	2.59	square kilometers	km^2
VOLUME				
fl oz	fluid ounces	29.57	milliliters	mL
gal	gallons	3.785	liters	L
ft^3	cubic feet	0.028	cubic meters	m^3
yd^3	cubic yards	0.765	cubic meters	m^3
NOTE: volumes greater than 1000 L shall be shown in m^3				
MASS				
oz	ounces	28.35	grams	g
lb	pounds	0.454	kilograms	kg
T	short tons (2000 lb)	0.907	megagrams (or "metric ton")	Mg (or "t")
TEMPERATURE (exact degrees)				
°F	Fahrenheit	5 (F-32)/9 or (F-32)/1.8	Celsius	°C
FORCE and PRESSURE or STRESS				
lbf	poundforce	4.45	newtons	N
lbf/in^2	poundforce	6.89	kilopascals	kPa

	per square inch			
LENGTH				
mm	millimeters	0.039	inches	in
m	meters	3.28	feet	ft
m	meters	1.09	yards	yd
km	kilometers	0.621	miles	mi
AREA				
mm^2	square millimeters	0.0016	square inches	in^2
m^2	square meters	10.764	square feet	ft^2
m^2	square meters	1.195	square yards	yd^2
ha	hectares	2.47	acres	ac
km^2	square kilometers	0.386	square miles	mi^2
VOLUME				
mL	milliliters	0.034	fluid ounces	fl oz
L	liters	0.264	gallons	gal
m^3	cubic meters	35.314	cubic feet	ft^3
m^3	cubic meters	1.307	cubic yards	yd^3
MASS				
g	grams	0.035	ounces	oz
kg	kilograms	2.202	pounds	lb
Mg (or "t")	megagrams (or "metric ton")	1.103	short tons (2000 lb)	T
TEMPERATURE (exact degrees)				
^oC	Celsius	1.8C+32	Fahrenheit	^oF
FORCE and PRESSURE or STRESS				
N	Newtons	0.225	poundforce	lbf
kPa	Kilopascals	0.145	poundforce per square inch	lbf/in^2

*SI is the symbol for the International System of Units. Appropriate rounding should be made to comply with Section 4 of ASTM E380.
(Revised March 2003)

ACKNOWLEDGMENTS

This work was funded by the National Highway Traffic Safety Administration under cooperative agreement DTNH22-10-H-00288 with the University of Michigan. The authors acknowledge the valuable contributions of Laura Malik to the study.

CONTENTS

EXECUTIVE SUMMARY

An exemplar THOR-05F was compared to the anthropometric specification from the Anthropometry of Motor Vehicle Occupants (AMVO) study on a wide variety of dimensions, including segment lengths, masses and CG locations; relative joint and landmark positions; and external body contours. Overall, the ATD matched the specifications well. Four potentially significant discrepancies were noted:

1. The upper-arm segment of the THOR-05F is shorter than the AMVO specification.

2. The shoulder cannot readily be placed into the driving posture represented by the AMVO contour, which might affect the realism of seat belt fit in some circumstances.

3. The THOR-05F buttock contour differs substantially from the AMVO contour, but the differences may represent an appropriate compromise given the differences between ATD and human flesh.

4. The jacket components representing breast tissue may not have sufficient positional control, potentially affecting belt routing and thoracic response.

Based on these observations, five recommendations were made:

1. Consideration should be given to lengthening the upper arm segment by 35 mm to better match the AMVO specification.

2. The static positioning of the shoulder components should be examined to determine if a more realistic driving posture could be created.

3. The vertical position of the ATD as installed in vehicle seats should be compared to the positioning of similar-size occupants to address the buttock contour concerns.

4. The effects of the jacket and breast components on belt routing relative to the pelvis, thorax, and shoulder should be examined to determine if greater control of the installation and positioning of these soft components is needed to ensure test repeatability and reproducibility.

5. Future ATD development efforts should include the provision of physical landmarks on the ATD to support anthropometric verification.

INTRODUCTION

THOR History

The THOR-05F ATD was developed under a NHTSA effort begun in the 1980s to create dummies with improved biofidelity and expanded injury assessment capabilities relative to the Hybrid-III ATD family (Shams et al. 2003, McDonald et al. 2003). The THOR-05F was designed using anthropometric data developed for the small adult female, nominally 5th percentile by both stature and weight, referencing the Anthropometry of Motor Vehicle Occupants (AMVO) study conducted at UMTRI in the early 1980s (Robbins 1983). The mechanical design follows that of the first generation midsize-male THOR ATD (THOR-50M-alpha), which preceded THOR-05F in development.

AMVO Small-Female Specification

In preparation for the current study, the question arose as to whether the 5th-percentile stature and weight values from the 1980s represent similar values relative to the current US adult population. Recently, Reed and Rupp (2013) analyzed data from the U.S. National Health and Nutrition Examination Survey to compare the nominal percentile values for the adult Hybrid-III ATD family to the current population. Table 1 lists selected stature and body weight percentiles for the U.S. population for three reference years. The 1974 values are equivalent to those used in AMVO. During the years 1974 to 2008, 5th-percentile female stature declined by 3 mm and 5th-percentile body weight increased by 3 kg. Neither change is likely to have a meaningful affect on ATD dimensions, indicating that an ATD developed to the 1974 reference dimensions (i.e., AMVO) would occupy the same position relative to the current population as it did in the 1980s.

Table 1
Percentiles of Stature and Body Weight for U.S. Adults (Reed and Rupp 2013)

Value	Stature (mm)			Body Weight (kg)		
Year	1974	1990	2008	1974	1990	2008
5th%ile Female	1511	1504	1508	47.3	47.8	50.3
50th%ile Female	1618	1618	1622	62.3	65.5	71.0
50th%ile Male	1753	1755	1761	77.0	79.8	85.4
95th%ile Male	1869	1880	1887	102.3	110.6	123.4

AMVO Small-Female Specification

The Anthropometry of Motor Vehicle Occupants (AMVO) project was funded by NHTSA and conducted by UMTRI to develop specifications for ATDs (Schneider et al.

1983). AMVO measured surface landmarks of 25 women close in size to the reference stature and body weight. Joint center locations were estimated from the surface landmark data with reference to previous cadaveric studies. Segment masses and centers of gravity were estimated based on previous studies of male cadavers (Robbins 1983).

Shams et al. (2003) and McDonald et al. (2003) describe the adoption of the AMVO small-female specification to the THOR-05F design. In general, the anthropometric targets were adopted without modification. However, the THOR ATD lacks many of the landmark points reported in AMVO, particularly those on the skin surface. Moreover, the THOR ATD design lacks many skeletal features that were referenced in the AMVO specification.

Evaluation Criteria

The purpose of the current work is to evaluate the size, shape, and mass distribution of an exemplar THOR-05F relative to human occupants who match the reference anthropometry for the ATD, and in particular to compare the THOR-05F to the AMVO small-female ATD specifications. The construction of the ATD was also considered relative to small female anatomy, including kinematic segment dimensions.

The ATD jacket was examined with reference to shape and installation. Based on previous issues with the chest jackets of the Hybrid-III small adult female (Tylko et al. 2006) and six-year-old child (Ebert-Hamilton and Reed 2011), the chest and breast areas of the jacket were closely examined relative to installation repeatability and potential effects on belt positioning.

Exemplar ATD

All measurements were conducted on a single THOR-05F obtained from NHTSA VRTC (Figures 1 and 2). The arms, forearms, and hands of the exemplar ATD were small-female Hybrid-III parts, as were the lower legs and feet. The THOR-05Lx was not part of the current evaluation.

Figure 1. A THOR-05F shown on the GESAC website (left) and the THOR-05F supplied for this study (right)

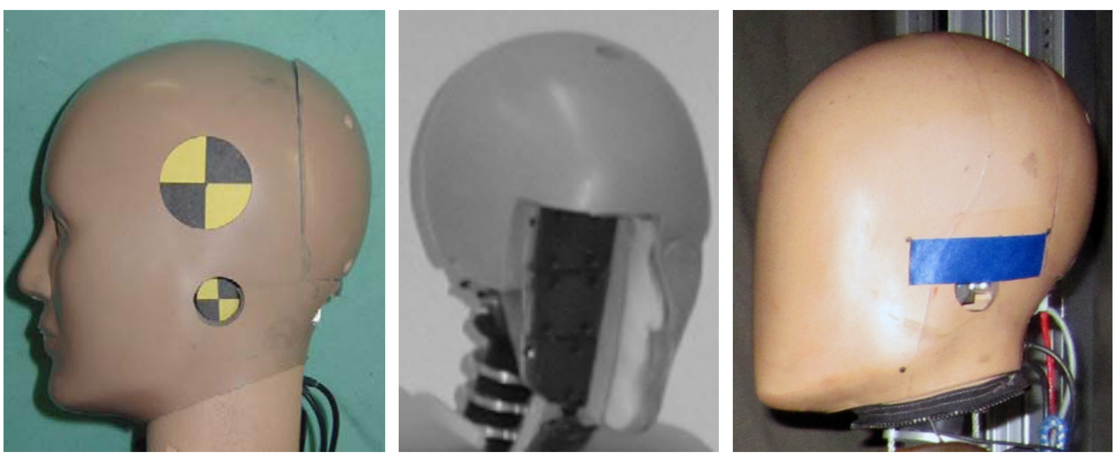

Figure 2. Images of the THOR-05F heads from the GESAC report (left), from the McDonald et al 2003 paper (middle) and the head supplied for this study (right).

METHODS

ATD Configuration

Table 2 lists the instrumentation configuration for the ATD as measured. The instrumentation wiring was supported separately, where possible, but the wiring introduces some uncertainty into the mass and CG values. The jacket was included in some measurements (see below) but removed for examination and to provide access to the ATD hardware. The THOR-FLx lower limbs, which were designed for the THOR-05F but can be retro-fitted to the HIII, were not supplied with the ATD. There are no arms specific to the THOR-05F; HIII arms were used on the exemplar ATD.

Table 2

THOR-05F Instrumentation on Exemplar ATD

Location	Sensor Type	As measured
Head	9 uniaxial accelerometers	No, but array fixture present
	1 Biaxial tilt sensor	Yes
Face	5 uniaxial load cells	Blanks
Neck	O-C joint rotary potentiometer	Yes
	Rear neck spring load cell	Yes
	Front neck spring load cell	Yes
	Upper neck load cell	Yes
	Lower neck load cell	Yes
Thorax	Thorax CG triaxial accelerometer	Blank
	4 CRUX units	Yes
Mid sternum	Uniaxial accelerometer	No
Upper Abdomen	Uniaxial accelerometer	No
Lower Abdomen	String potentiometer (L&R)	Yes
T-1	Triaxial accelerometer	Yes
T-12	Accelerometer	Yes
	Load cell	Yes
Pelvis	Pelvis CG triaxial accelerometer	No
	Acetabulum Load cell (L&R)	Yes
	Iliac spine load cells (L&R)	No
Femur	Load cell (L & R)	Yes
Knee	Shear displacement (L&R)	Yes
Lower Leg	THOR-FLX instrumentation	No
Foot	Foot accelerometer (L&R)	Blanks

Segment Mass and Center-of-Gravity (CG) Location

The limb segments were disassembled and weighed using load cell scale (Medweigh MS-4600). CG location was computed using the hanging and balance table methods shown in Figure 3. To find the longitudinal location of CG within a limb segment the segment was balanced on a tilt table. Limb segments were suspended to locate the CG in a second plane. The planes defined by these two methods were marked on 4 sides of the segment and digitized during scanning (Figure 4). The intercept of the lines connecting the marks on the opposite sides of the segment was considered the CG location.

Figure 3. Balance table (left) and hanging (right) methods for measuring limb segment center of mass.

Figure 4. An example of CG marks drawn over in the photo suspended (solid) and balance table (dashed) CG methods illustrated on upper arm segment.

Landmark Measurement

The ATD lacks specific points that are intended to be directly homologous to most of the available surface landmarks. Similarly, reference points that can be readily used to identify joint locations are not available. Consequently, a detailed investigation of the physical ATD and the design specifications for both the THOR-05F and THOR-50M was conducted to establish appropriate points for comparison. Tables 3-8 describe the reference points that were defined by body region. For hinge joints (wrist, knee, elbow, head/neck) the joint center location was estimated to lie on the hinge axis at the centerlines of one or both of the adjacent segments, or on the body midline. Ball joint center locations (hip and ankle) were estimated by fitting spheres to points digitized on the ball hardware. The "centers" of flexible joints (lumbar, mid-thorax, and neck) were estimated at the center of the corresponding cylindrical component. Some of the AMVO spine joint locations do not correspond directly to points used in the THOR-05F design. Instead, locations of the desired joints were estimated from the location of other joints reported in the AMVO documentation. In these cases, the same procedures as used in the development of the THOR-05F were used in the current study to estimate the joint locations.

Head and Neck – According to the GESAC report during development of the THOR-05F, a H-III head casting was chosen as the basis for casting the shape of the THOR-05F. The drawings of the HIII 5th female head were compared to the AATD 5th female head and aligned on the OC joint. The H-III was set with the lower machined surface of the head casting rotate about 2.5 degrees down from horizontal so that the ATD face hit the glabella and gnathion of the AATD. The head geometry was modified to create a head casting with a plate for face load cells. The head casting and head neck mounting platform were designed such that the head casting would lie within the AATD shell using the OC point as the reference. During development, a ballast was added on the superior surface of the interior of the head to meet the target CG. Figure 5 shows the ballast inside the head supplied for this study.

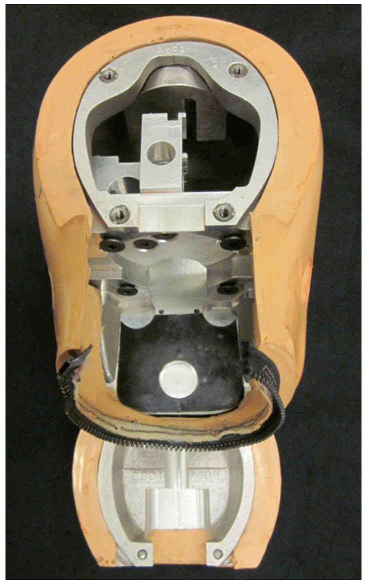

Figure 5. Head of THOR-05F supplied for this study.

Table 4 shows the location of the neck and other spine joint measured. For measurements at load cells, points digitized around the outside were used with reference to load cell diagrams to calculate the center of the neutral plane.

Table 3
Head Landmarks and Joints

AMVO comparison	Description
Head Plane	The plane described by the infraorbitale and tragion is anatomical position of the skull. The head of the THOR-05F did not have infraorbintale or tragion marked. Therefore the orientation of the instrument shelf was measured and translated to the exterior surface and marked with 2 points. 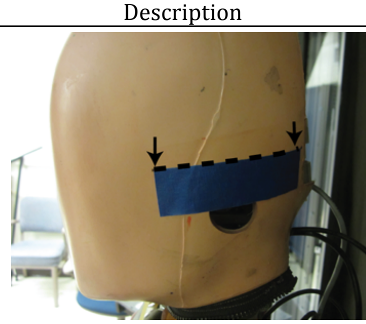 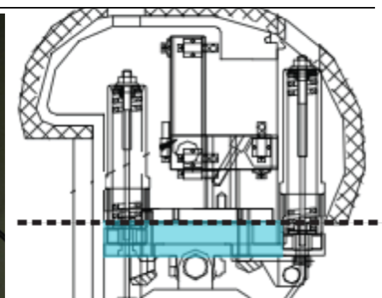
Head/Neck Joint	The center of the ATD O.C. pin was digitized on the left and right side of the ATD. The head-neck joint was calculated as point along this vector at the centerline of the head. 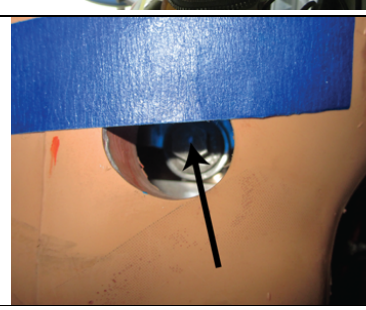 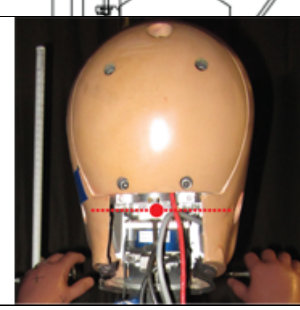

Table 4
Spine Landmarks and Joints

AMVO Comparison	Description
Lower Neck (C7/T1) Joint	A point on the anterior surface of the neck between the bottom two neck bucks as described in theHuang et al. 2003 on the development of the THOR-50th head-neck system 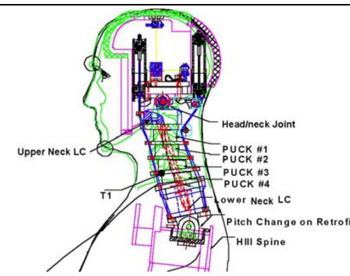
	The center of the flex joint was found by digitizing points at the top and bottom of the neck and calculating the center. 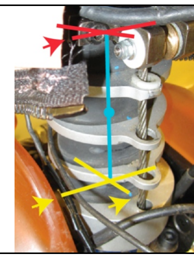
Estimate of T3/T4 Joint	Neck pitch change mechanism 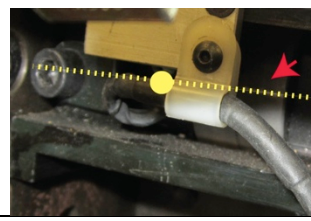 The pitch change mechanism was not accessble for digitizing. The center was estimated as a center of rotation of the neck relative to the thorax.
Estimate of T7/T8	A flex joint was added to the THOR design to provide additional flexibility to the thorax. Points were taken around the outside of the joint that were used to calculate the center 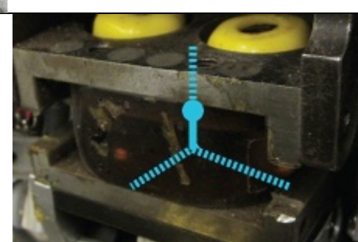
Thoracic (T12/L1) Joint	According to the THOR-50th manual, the lower thoracic spine pitch change mechanism is centered at the approximate location of the anthropomorphic landmark defined by the T11/T12 joint. The centers of either side of the mechanism were digitized. The point along this vector at the ATD midline was considered the joint 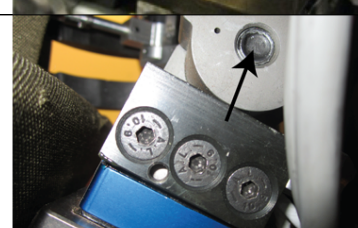
Lumbar Joint L2/L3 or L5/S1	Center of the flexible lumbar spine at the top and bottom calculated from points digitized at around the circumference 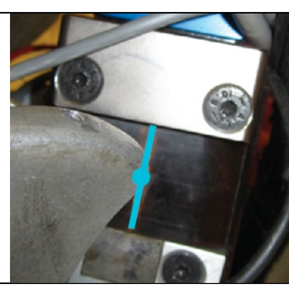 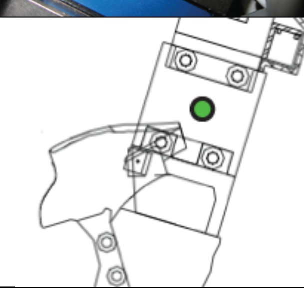

Table 5
Pelvis Landmarks and Joints

AMVO Comparison	Description		
Hip Joint (midpoint between right and left hip joint centers)	Center of the hip ball volume, digitized by taking points around sphere and verified by calculating the center of the hip socket	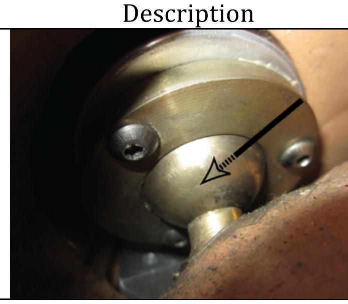	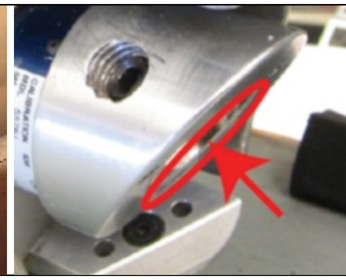
Anterior Superior Iliac Spine (ASIS), Pubic Symphysis (PS), Ischial Tuberosity (IT)	ASIS and PS (yellow and black arrows) were reachable with the pelvis flesh on the ATD. These points were used to track the hips and L5/S1 joint.  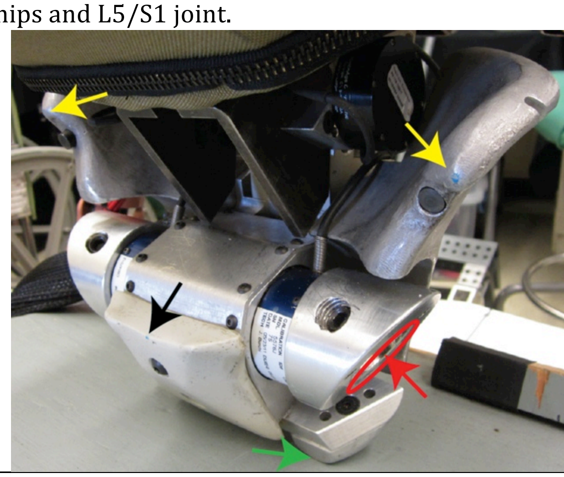		

Table 6
Lower Limb Landmarks and Joints

AMVO Comparison	Description		
Knee Joint	Mid point of leg and pivot point	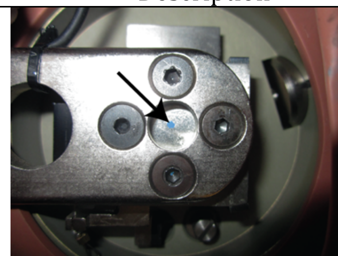	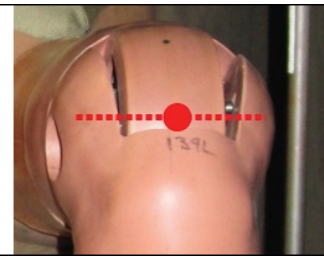
Ankle Joint	Center of ball joint		

Table 7
Upper Limb Landmarks and Joints

AMVO Comparison	Description		
Sterno-Clavicular Joint		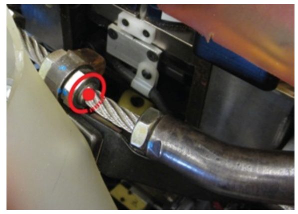	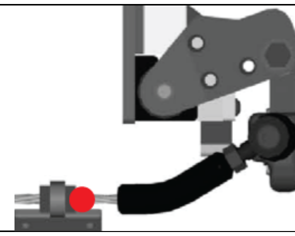
Shoulder Joint	Red = flexion-extension, and abduction-adduction Yellow, blue and and other blue more medial are rotation	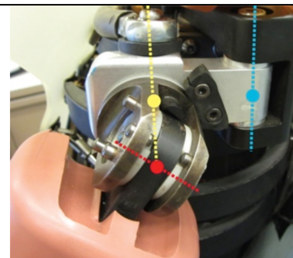	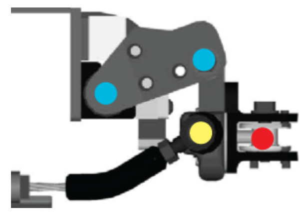
Elbow Joint	Center of elbow hinge	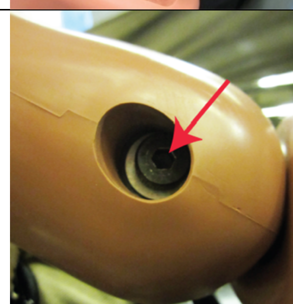	
Wrist Joint		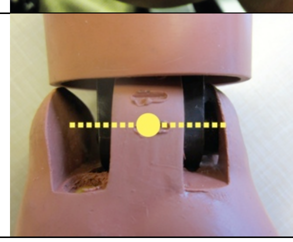	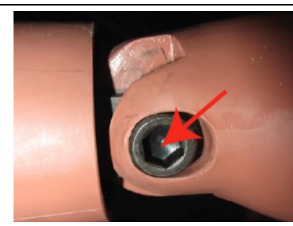

Table 8
Torso Landmark Definitions.

AMVO Comparison	Description	
Suprasternale	The most superior-anterior point on sternum	
C7	Recorded both the top of lower neck load cell and center of ATD Rib "1" along posterior midline	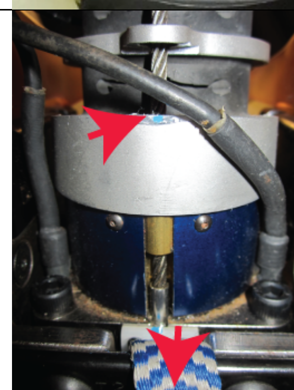
10th Rib	Most lateral point on center of ATD Rib "7"	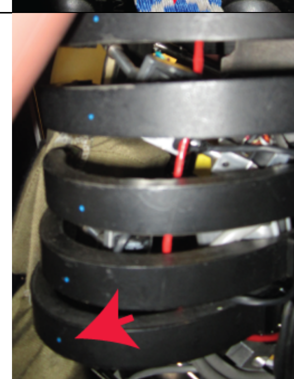
T12	Center of ATD Rib "7" along posterior midlie	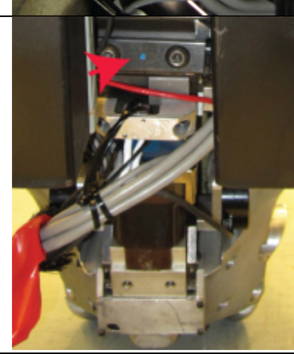

Surface Contour Using 3D Scanning

The ATD without jacket was positioned in a posture similar to that of the AMVO dataset. Figure 6 shows the ATD in the scanning posture. The aim was to match joint angles and surface shape as closely as possible. The ATD surface was then scanned using a full-body laser scanner (Vitus XXL) and a hand-held structured-light scanner (Artec Eva). Landmarks were digitized using a coordinate measurement machine (FARO Arm) on the surface of the ATD as were other reference points such as the CG marks and reference points to align segments later. Surfaces that could not be reached by the scanner while the ATD sat, including under the legs and feet and along the spine, were scanned with the ATD in a different position. Reference points located in each scanned position were used to combine the data using 3D imaging software (Geomagic 12). Joint centers locations were calculated and segment lengths measured.

Jacket

The jacket has an unusual construction, relative to other ATD jackets and clothing. The jacket construction was examined and documented with particularly attention to the jacket fit and the contour in the areas of belt interaction. The ATD was scanned with and without the jacket to quantify the additional contour generated by the jacket. The jacket was examined separate from the ATD and the jacket installation process was performed several times to identify issues that might affect jacket positioning and the resulting ATD contour and belt interaction.

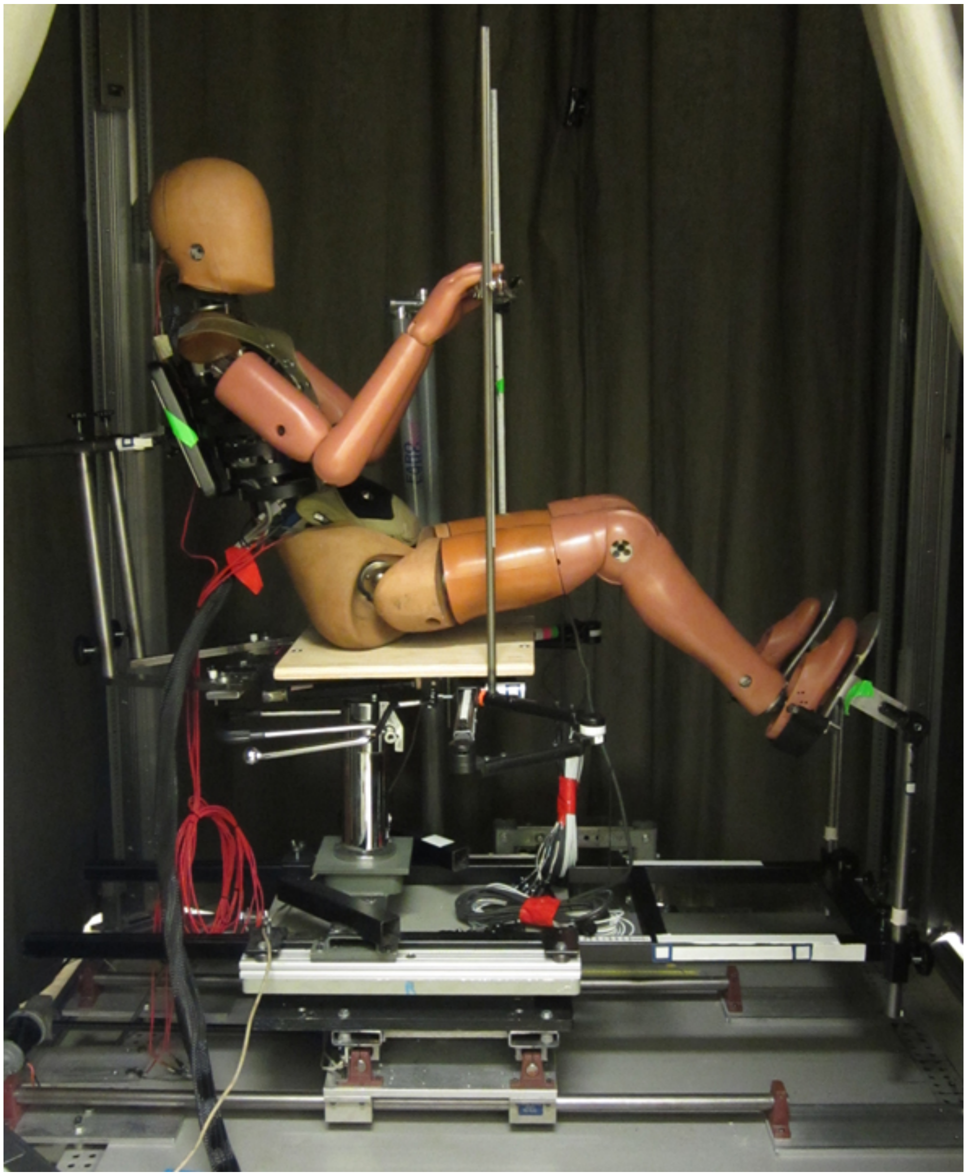

Figure 6a. ATD in VITUS XXL laser scanner, showing positioning fixtures.

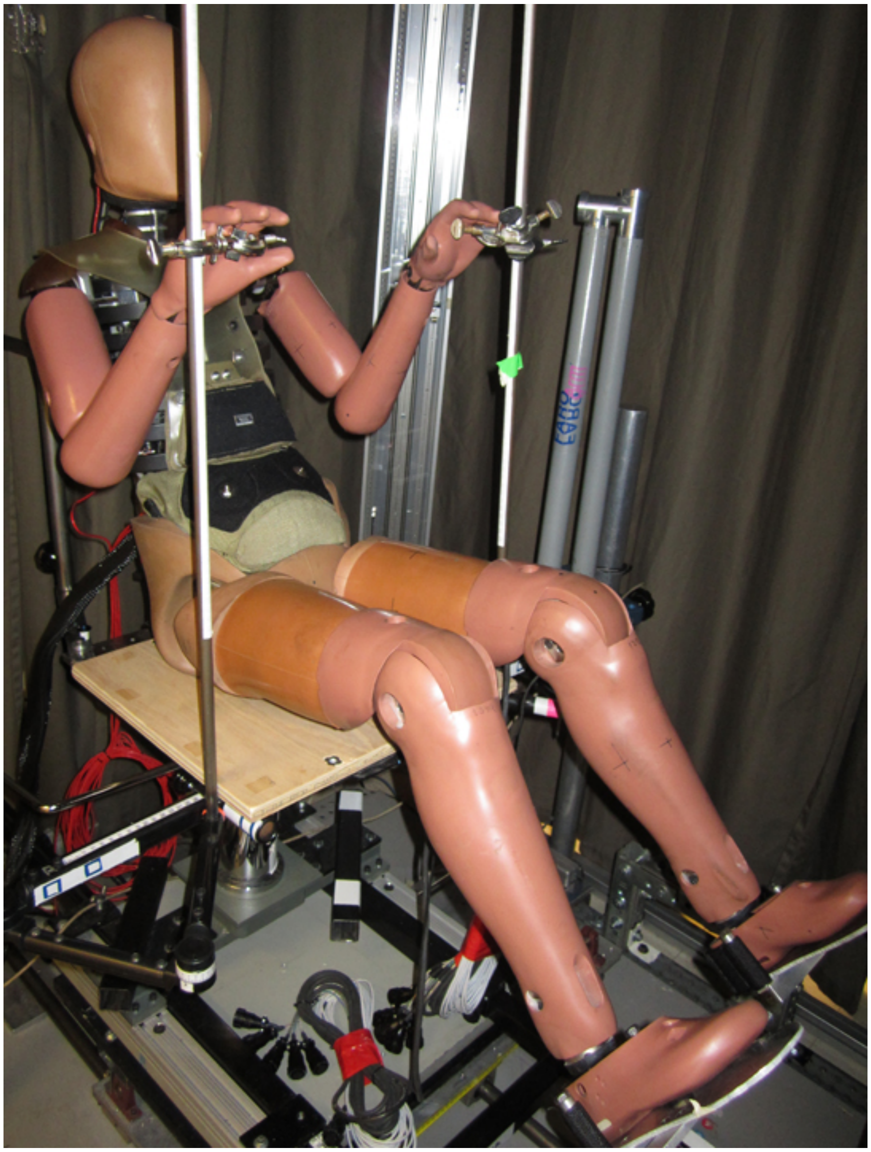

Figure 6b. ATD in VITUS XXL laser scanner, showing positioning fixtures.

RESULTS

Segment Mass

Total weight of the ATD with current instrumentation was 49.6 kg plus 1.25 kg for the jacket (total 50.25 kg). This value exceeds the AMVO reference of 46.9 kg (mean of the small-female AMVO subjects) by 3.35 kg (7.1%), although it matches well with the current 5th-percentile female value for the U.S. population (see Table 1). Table 9 lists the masses of the extremity segments along with the AMVO targets. Note that the comparisons are hampered by differences in flesh segmentation between AMVO and the ATD. The largest discrepancy was observed in the lower leg, with the THOR-05F exceeding the AMVO target by 38 percent.

Table 9
Segment Masses

Segment	AMVO Target Mass (kg)*	THOR-05F Mass (kg)	Ratio	Segment as Weighed
Upper Arm	1.124	1.10	0.98	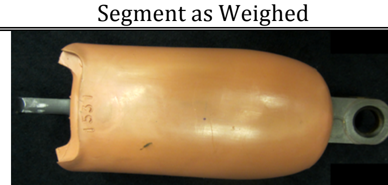
Lower Arm		0.75		
Hand		0.25		
Lower Arm + Hand	1.138	1.00	0.88	
Upper Leg	5.914	4.95	0.84	
Lower Leg	2.360	3.25	1.38	
Foot	0.638	0.70	1.10	

Extremity Segment Lengths

Table 10 lists the measured extremity segment lengths (between joint centers) along with the comparative values from AMVO. The lengths of two segments differed markedly from the AMVO values. The upper arm (shoulder to elbow) was 39 mm (15%) shorter than the AMVO value, and the lower leg was 27 mm (8%) shorter.

Comparisons of torso segment lengths were more difficult because only the hips and head/neck joint are well defined. Table 11 lists the segment lengths from AMVO based on joint-to-joint distances, along with the ATD points used to approximate the joint locations.

Table 10
Limb Segment Lengths

	Length (mm)				
Segment	AMVO	THOR	THOR-AMVO	THOR/AMVO	Measured from center of joint
Upper Arm	**257**	**218**	**-39**	**0.85**	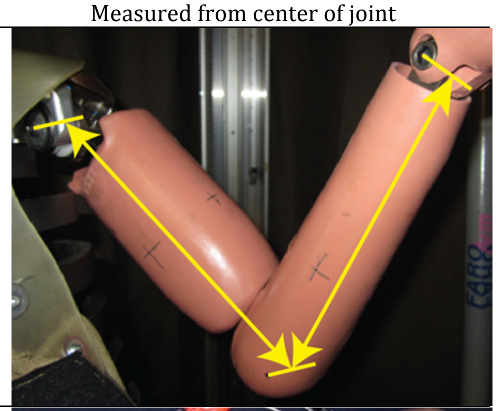
Lower Arm	229	214	-15	0.94	
Upper leg	377	375	-2	0.99	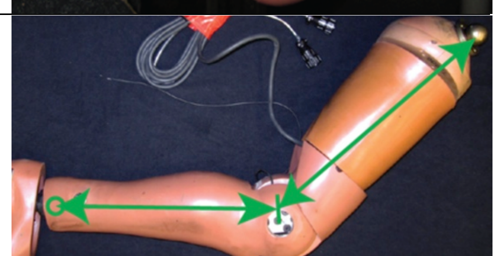
Lower leg	342	315	-27	0.92	
Foot	215	220	5	1.02	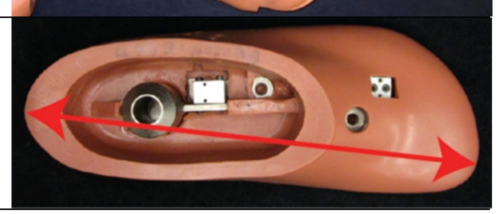

Table 11
Torso Segment Lengths

AMVO Segment	Spine Length (mm)	Length (mm)	THOR-05F Segment	Spine Length (mm)	Alternate Lengths (mm)	THOR/ AMVO
Hip Joint to L2/L3		153	Hip joint to center of lumbar flex joint	118		0.77
Hip Joint to L5S1	92					1.28
			Hips joint to bottom-center of lumbar flex joint		108	1.17
Hips to T12L1		204	Hips to thorax pitch change mechanism		212	1.04
L5S1 to T12L1	117		Center of lumbar flex joint to thorax pitch change mechanism	103		0.88
			Bottom-center of lumbar flex joint to thorax pitch change mechanism		117	1.00
T12L1 to C7T1	291		Thorax pitch change mechanism to Huang T12	285		0.979
			Thorax pitch change mechanism to neck pitch change mechanism		196	0.68
			Thorax pitch change mechanism to center of neck flex joint		298	1.03
C7T1 to Head/Neck	90		Huang T12 to head/neck joint	93		1.03
			Neck pitch change mechanism to head/neck joint		194	2.15
			Center of neck flex joint to head/neck joint		83	0.92
Sum	590			599		

Center-of-Gravity (CG) Location

Table 12 presents the measured longitudinal center of gravity location for the extremity segments with the AMVO targets. The dimensions are reported along the line connecting the proximal and distal joint centers, relative to the proximal joint. Because the segment lengths differ from AMVO, the CG locations are also reported as a percentage of the segment length. The only substantial discrepancy is observed with the upper-arm segment, probably due in part to the unexpectedly short segment length.

Table 12
Location of Segment Center of Gravity

Segment	Distance from	Along Vector Between	AMVO CG (mm)	A: AMVO CG/Segment Length	THOR CG (mm)	B: THOR CG /Segment Length	**B/A**
Upper Arm	Shoulder F/E A/A Joint	Shoulder Joint to Elbow Joint	112*	0.44	113	0.52	1.18
	Shoulder Rotation Joint	Shoulder Joint to Elbow Joint	112*	0.44	158	0.60	1.38
Upper Arm	Elbow Joint	Elbow Joint to Shoulder Joint	**145**	**0.56**	**106**	**0.48**	**0.61**
Lower Arm	Elbow Joint	Elbow Joint to Wrist Joint			87	0.64	
Lower Arm + Hand	Elbow Joint	Elbow Joint to Wrist Joint	140	0.36	138	0.37	1.03
Upper Leg	Hip Joint	Hip Joint to Knee Joint	152	0.40	169	0.45	1.12
Lower Leg	Knee Joint	Knee Joint to Ankle Joint	149	0.44	142	0.45	1.03
Foot	Heel	Heel to Toe	84	0.39	100	0.45	1.16

*Same point in human, two mechanisms in THOR

Table 13 lists the measured head center of gravity relative to head relative to O.C.

Table 13
Location of Head Center of Gravity

Origin @ O.C.	AATD 5% Female*	HIII 5F (derived from drawings)*	Thor 5F unbal-lasted*	Thor 5F predicted after ballasting*	McDonald**	This study THOR-5F measured
X coordinate (mm)	5	20	13.5	11	11	6
Z coordinate (mm)	59	43	43	47	49	51
Head Mass (kg)	3.70	3.73	3.5	3.7	3.66	3.25

* GESAC Report
**McDonald et al. 2003

ATD Settings and Landmark Measurement

The landmarks described in Tables 4-7 were digitized using a FARO Arm with the ATD placed in a posture approximating the AMVO posture. The upper and lower pitch change mechanisms had lines marking several settings, but the GESAC report did not document their meanings and they were different than the lines documented in the THOR-50th percentile manual. Therefore the settings are reported here as included angles. The included angle (Head/Neck Joint – upper (neck) pitch change mechanism-lower thorax pitch change mechanism) at the upper pitch change mechanism as scanned was 157˚ as shown in Figure 7. The head and neck were then rotated 6 degrees to match the Head/Neck joint location of the AMVO posture resulting in an included angle of 151˚ or 139˚ as measured to T1 Joint (Huang et al 2003). The neck cables can be adjusted to alter the curvature of the neck and hence the head position relative to the thorax. Measurements were conducted with the cables in the as-received condition. The lower thorax pitch change was set to an included angle (neck pitch change mechanism-lower thorax pitch change mechanism-center of lumbar flex joint) of 170˚.

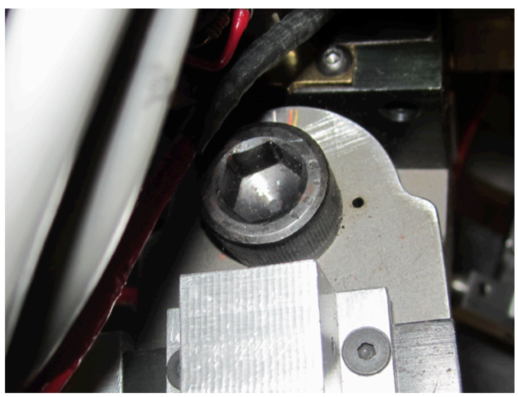

Figure 7. Lower pitch change mechanism setting during scanning.

Table 14 compares the measured locations with the corresponding points in AMVO. Prior to comparison, the AMVO points were adjusted using rigid body transformations (e.g., rotating and translating the forearm at the elbow prior to comparing hand landmarks). When a homologous point was not available, one or more approximating points were digitized, as described in the table.

Table 15 compares pelvis dimensions with AMVO, Reynolds et al. (1981), and McDonald et al. (2003), who presented target values for the THOR-05F. In all cases, the measured THOR values are within 10 mm of the AMVO values.

Table 14a
Coordinates of THOR-05F Points relative to AMVO with Similar Postures

AMVO Point	Coordinate (mm)		THOR-05F Point	Coordinate (mm)		Difference	
	X	Z		X	Z	X	Z
PS	44	22	Anterior-superior edge of plastic	44	18	0	-4
Hip Joint	0	0	**Mid point between hip joints**	0	0	**0**	**0**
L5/S1 Joint	-80	46					
			Center of lumbar flex joint	-104	57		
L2/L3	-121	102					
			Lumbar load cell	-127	102		
T12/L1 Joint	-149	140	**Lower thorax pitch change mechanism**	-152	148	**-3**	**8**
T8/T9 Joint	-196	273					
T7/8 Estimate*	**-193**	**302**	**Center of mid-thorax flex joint**	**-192**	**244**	**1**	**-58**
T4/T5 Joint	-205	381					
T3/T4 Estimate**	-199	391	**Neck pitch change mechanism**	-221	332		
Sternum Top	-144	391	Sternum Top	-146	393	-2	2
C7 Process	-238	445	Posterior rib “1”	-258	346	-20	-99
			Top-back edge of lower neck load cell	-243	407	-5	-38
T12 Process	-200	122	Posterior rib “7”	-198	158	2	36
C7/T1 Joint	-183	429	**T12 Huang 2003 (anterior midpoint of pucks 3 and4)**	-185	431	**-2**	**2**
			Neck pitch change mechanism	-221	332		
			Lower neck load cell	-216	372		
			Center of neck flex joint	-205	442		
			Upper neck load cell	-197	496		
Head/Neck Joint	-189	519	**Head/neck joint**	-194	524	**-5**	**5**

* T4/T5P1 = (Normalized T8/T9 –T4/T5)*81.5 mm (3.21 in) +T4/T5 =(-198, 300)
T4/T5P1 Estimate = (Normalized vector perpendicular to T/T9-T4/5)*5.08mm (2.1 in) + T4/T5P1 =(-202,301) or (-193 ,302) as the text does not indicate direction (FROM GESAC)
** C7/T1 to T4/T5 distance= 47 mm , 47 mm / 4 segment =11.8 mm/seg
(Normalized T4/T5-C7T1)* (3*11.8)+C7/T1 =(-199,391)

Table 14b
Coordinates of THOR-05F Points relative to AMVO with Similar Postures

AMVO Point	Coordinate (mm)			THOR-05F Point	Coordinate (mm)			Difference		
	X	Y	Z		X	Y	Z	X	Y	Z
	-	-	-	Trochanter Load Cell	0	46	0	-	-	-
ASIS	-15	103	75	ASIS	-14	107	74	1	4	-1
Left Hip	0	80	0	Center of ball joint	0	80	0	0	0	0
Inferior tuberosity point	24	48	-56	Anterior-inferior edge of ischial tuberosity	21	48	-60	-3	0	-4
Frankfort Plane	-	-	-	-	-161	62	550	-	-	-
Frankfort Plane	-	-	-	-	-238	53	550	-	-	-
Infraorbitale	-103	32	550	-	-	-	-	-	-	-
Tragion	-180	67	545	-	-	-	-	-	-	-
Sternoclavicular Joint	-146	17	389	Sternoclavicular Joint	-151	10	388	-5	-7	-1
10th Rib Lateral	-96	129	125	Lateral rib "7"	-124	125	164	-28	-4	39
Glenohumeral Joint	-174	146	354	Shoulder Flex-Ext Joint	-186	155	352	-12	9	-2
Elbow Joint	20	179	188	Elbow Joint	-25	179	205	-45	0	17
Wrist Joint	134	155	385	Wrist Joint	89	168	387	-45	13	2
Knee Joint	363	75	71	Knee Joint	362	77	64	-1	2	-7
Ankle Joint	593	86	-182	Ankle Joint	574	86	-169	-19	0	13
Toe	729	126	-75	Toe	716	79	-61	-13	-47	14
Heel	618	90	-254	Heel	603	85	-250	-15	-5	4

Table 15
Comparison of Pelvis Dimensions

	Reynolds*	AMVO	McDonald**	Measured	THOR-AMVO
L. hip to R. hip	157.5	160	157.5	159	-1
L. ASIS to R. ASIS	218	206	216.7	215	9
L. hip to L. ASIS	78.2	80	79.4	81	1
R. hip to R. ASIS	72.3	80	80.6	84	4
L. hip to L Isch. Tuberosity	69.6	69	70.9	70	1
R. hip to R Isch. Tuberosity	77.1	69	70.9	71	2

*Reynolds et al. 1981

**McDonald et al. 2003

Surface Contour Using 3D Scanning

The scan data were used to compare the exterior contours of the ATD with the reference AMVO shell. We used a digital version of the shell obtained from laser-scan data of the physical shell constructed during the AMVO project. The physical shell was developed to closely match the mean landmark values obtained from the small-female cohort in a driving posture. Importantly, the shell was constructed based on body contours obtained with the subjects sitting in a contoured hardseat that was developed based on measurements of the deflected surface contour of automotive seats. In constructing the shell, the human contour in the areas contacting the hardseat were assumed to match the hardseat surface.

Figure 8 shows the AMVO and THOR-05F scan data overlaid with transparency to facilitate comparisons. The immediate impression is that the overall size and posture of the ATD are close to the AMVO reference. However, several discrepancies are apparent. Referring to Figure 8b, the rear-view profile of the buttock area differs substantially. The AMVO contour represents the deformed contour of a sitter on a contoured hard seat, which is reasonably representative of the deformed contour of a sitter on deformable automotive seat. In contrast, the ATD is markedly narrower at the hips and thighs, and the buttock flesh protrudes rearward more near the seat surface.

Because the alignment of the 3D data affects the apparent discrepancies, several alternative alignments were used to facilitate the comparison. Figure 9 shows the AMVO shell and ATD scan using three alignments. The results confirm the findings from other measurements that the overall size of the ATD matches the AMVO reference closely, and that the ATD is capable of achieving the AMVO posture, with one exception: The resting position of the ATD shoulder joint is more rearward relative to the thorax than the shoulder of the AMVO shell. The AMVO posture is a driving posture with the hands supported; the THOR-05F posture may be more representative of the shoulder posture with relaxed upper extremities. However, we note that it was not feasible to pull the THOR-05F shoulders into a static posture to match the driving posture of the AMVO shell.

Figure 10 shows a dimensioned image of the AMVO and THOR shapes in the buttock region. Figure 11 shows a map of the deviations after aligning on the hip joint center and rotating around the hip axis to align the vector from the hips to L5/S1. The THOR-05F is approximately 66 mm narrower at the hips than the AMVO shell. The bottom of the buttock contour is also markedly more angular than the AMVO shell. Note that the THOR contour was scanned undeflected (ATD lying on its side) whereas the AMVO contour is intended to represent the contour of the sitter on a padded vehicle seat, although the shape above the seat surface is based on subjects sitting in a contoured hardseat. The buttocks were scanned unsupported and then merged with the rest of the scan. The amount of compression at the buttock in the seated posture was measured to be only 3 mm.

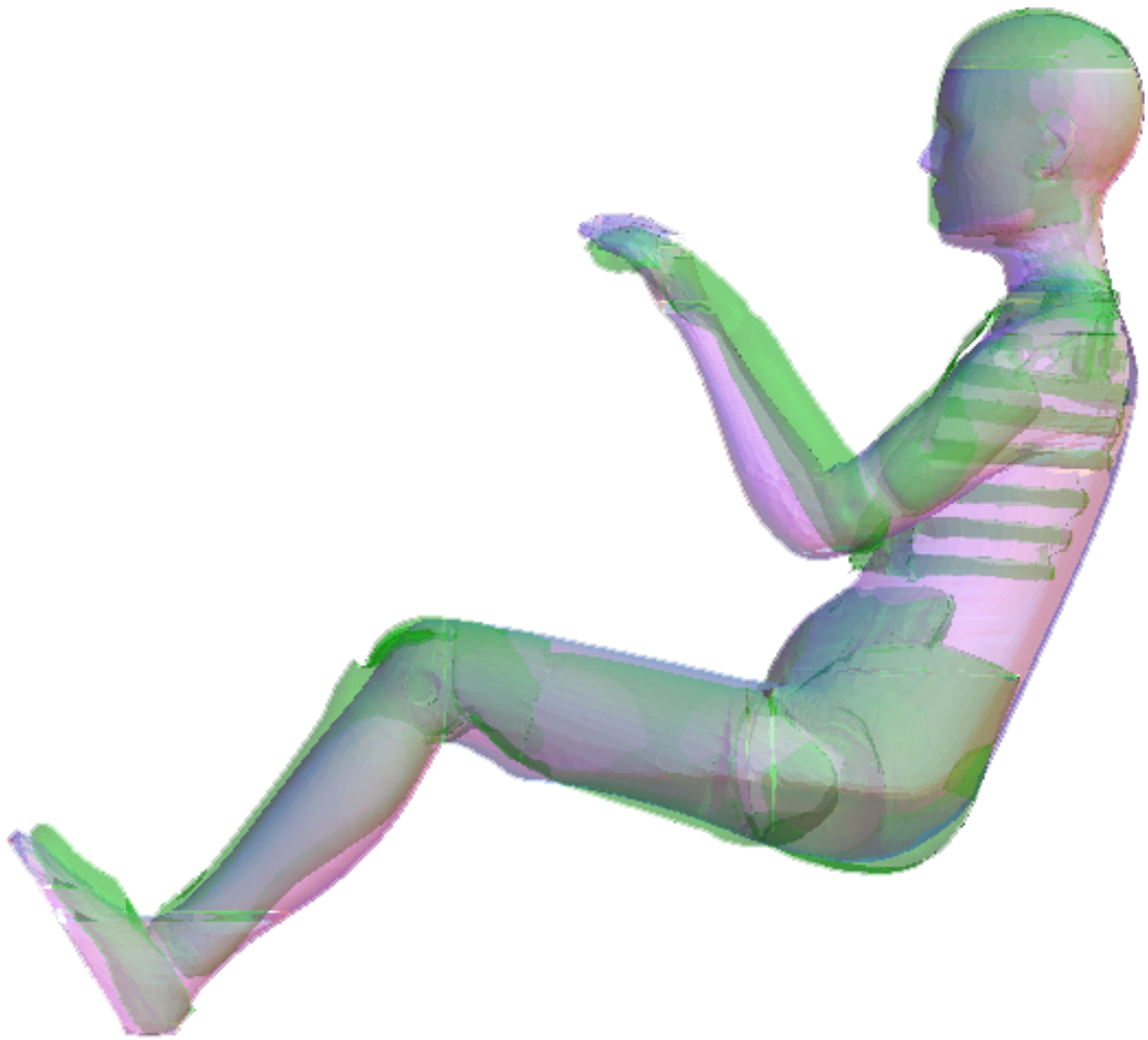

Figure 8a. THOR-05F 3D contour (green) overlaid with the AMVO small-female shell (pink, transparent), aligning at the back and bottom of the pelvis.

Figure 8b. THOR-05F 3D contour (green) overlaid with the AMVO small-female shell (pink, transparent), aligning at the hip joint location.

Figure 9. THOR-05F (green) and AMVO (pink) with THOR-05F as scanned (left), aligned to AMVO on hip location (middle) and aligned on hip location and then rotated 3 degrees forward (right).

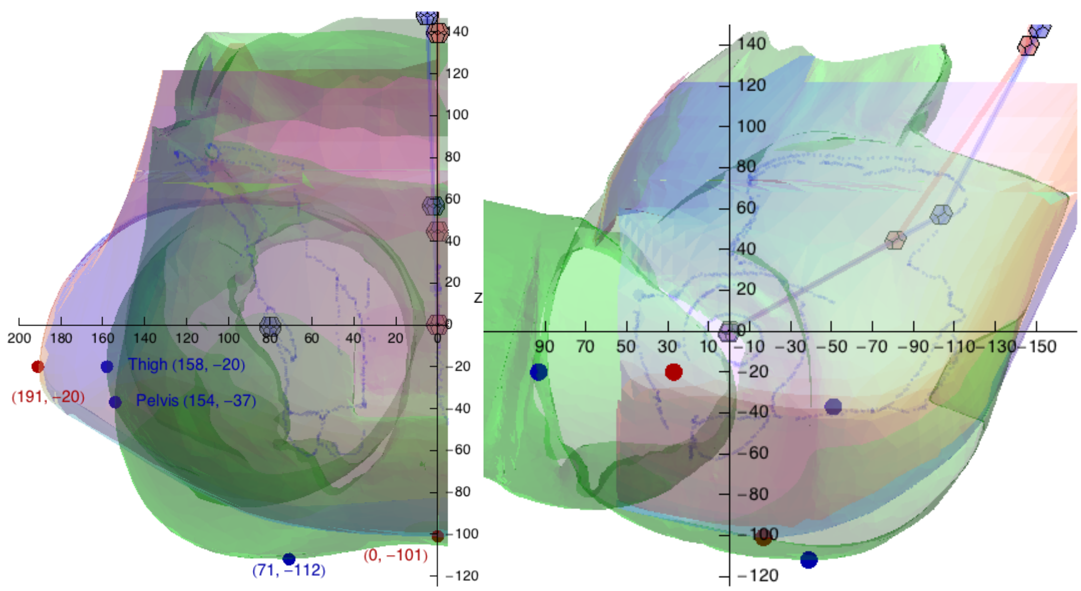

Figure 10. Dimensioned view of AMVO (pink) and THOR-05F (green) contours in the buttock area.

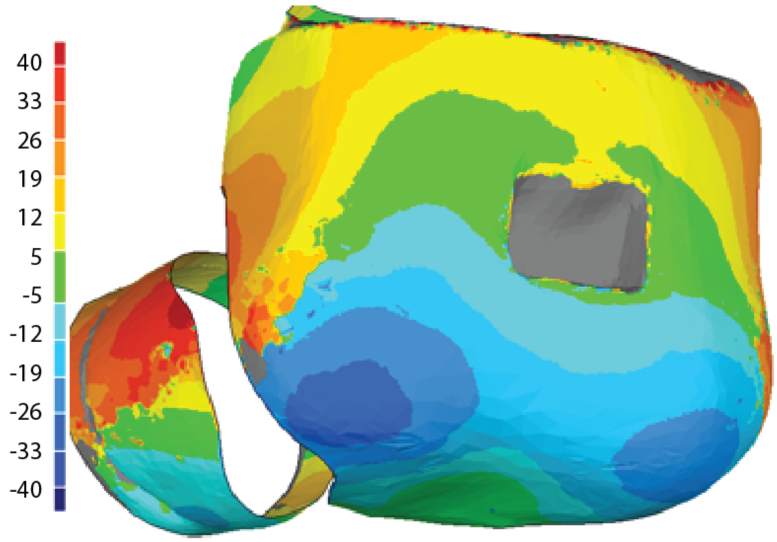

Figure 11. Map of the deviations between the AMVO and THOR-05F surfaces in the buttock area. Colors denote deviation levels in mm. Positive values indicate that the AMVO surface is outside of the THOR-05F surface.

Spine Linkage

A series of analyses were conducted to compare the AMVO description of the dimensions and posture of the spinal column with the THOR-05F. Figure 12 shows the set of points chosen to compare between the two datasets. Note that the THOR specification lacks specific anatomically referenced spine landmarks between the hip and the base of the head. The “neck” of the ATD is markedly longer than the cervical spine of the human, due to the ATD design decisions necessary to accommodate the neck instrumentation. The THOR-05F neck design is based on the THOR-50M Beta neck. The report by Huang (2003) on the THOR male Beta neck explains that the longer neck was needed for biofidelic response in dynamic flexion and extension. To achieve an acceptable anthropometric neck length, the “T1” was located at the anterior neck column between the bottom neck 2 pucks. The neck pitch change mechanism is located at approximately T3/T4, whereas the top of the neck (approximately the atlanto-occipital joint) can be aligned very closely with AMVO. Figures 13 and 14 show the analogous spine points (see Table 4 for definitions) along with the contours from scanner data. Three alternative alignments are shown, demonstrating that the ATD spine posture can be made to correspond closely with the AMVO targets.

Figures 14 and 15 show the whole skeletal linkage for AMVO and the ATD, after articulating the segments within the ATD range of adjustment to maximize the correspondence. The most apparent discrepancy is that the ATD upper-arm segment is substantially shorter than the AMVO reference.

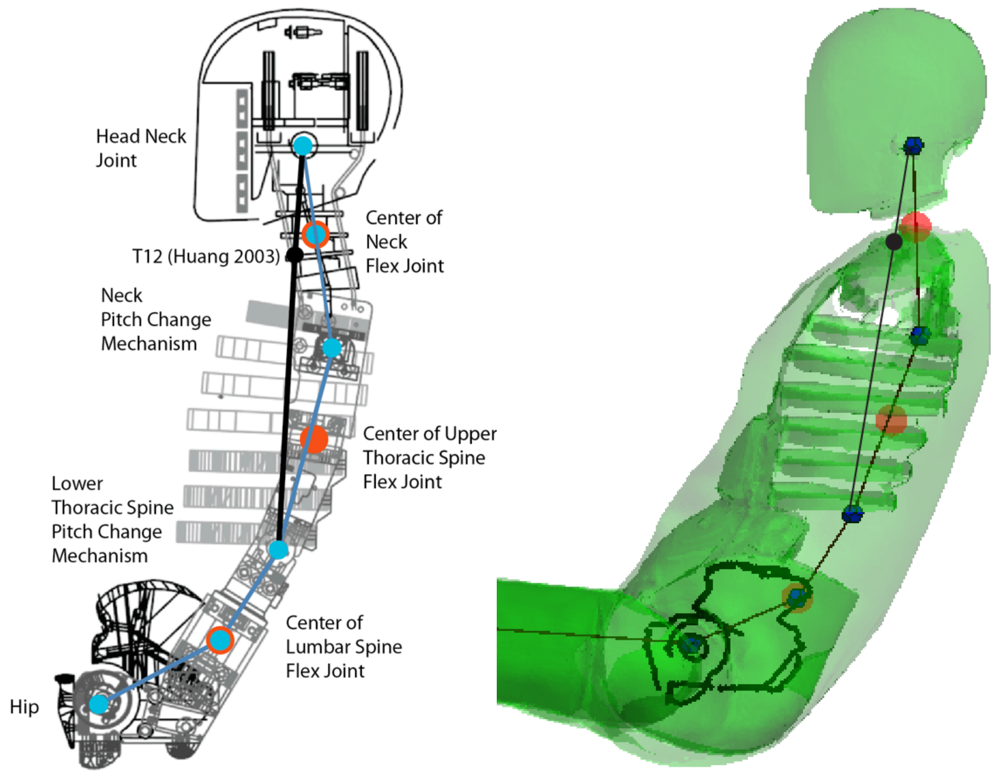

Figure 12. Linkage points digitized on THOR-05F drawn on CAD illustration (left) and plotted to-scale on the scan (right) from this study

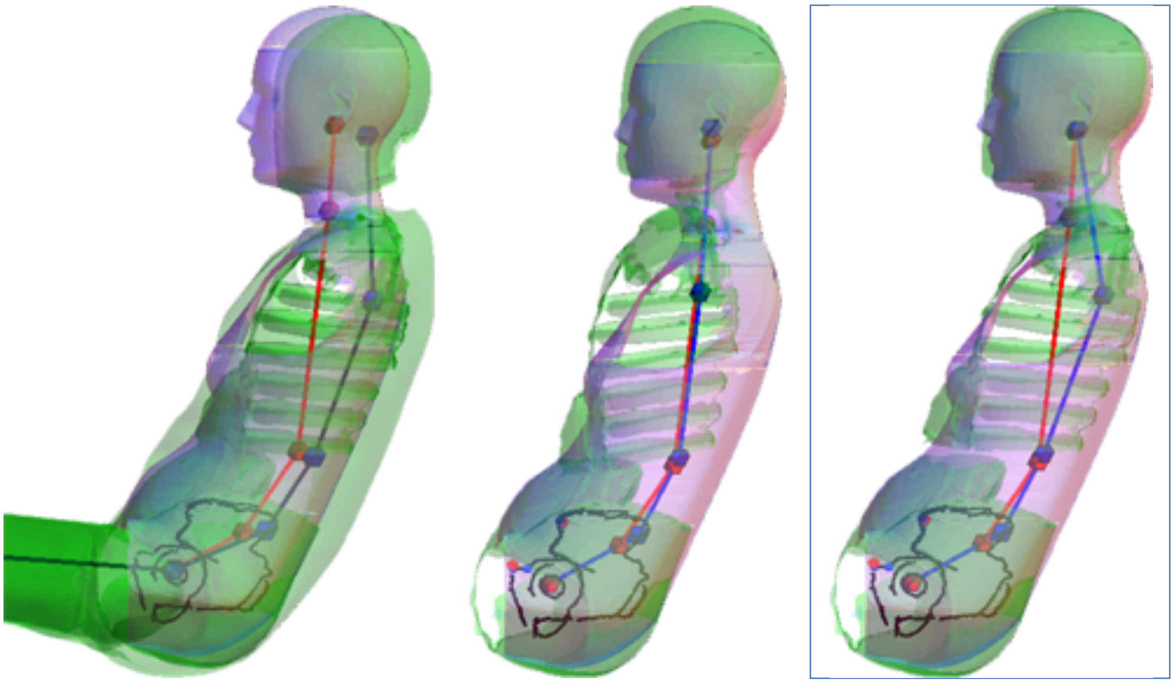

Figure 13. THOR-05F surface (green) and spine (blue) and AMVO (pink) surface and spine (red) with THOR-5F spine set as scanned (left), with spine segment angles matching AMVO posture (middle), and with pelvis and lumbar matching AMVO (red points are AMVO ASIS and PS), but with neck rotated 6 degrees (2 indents) forward so the head joint comes close to AMVO value (right).

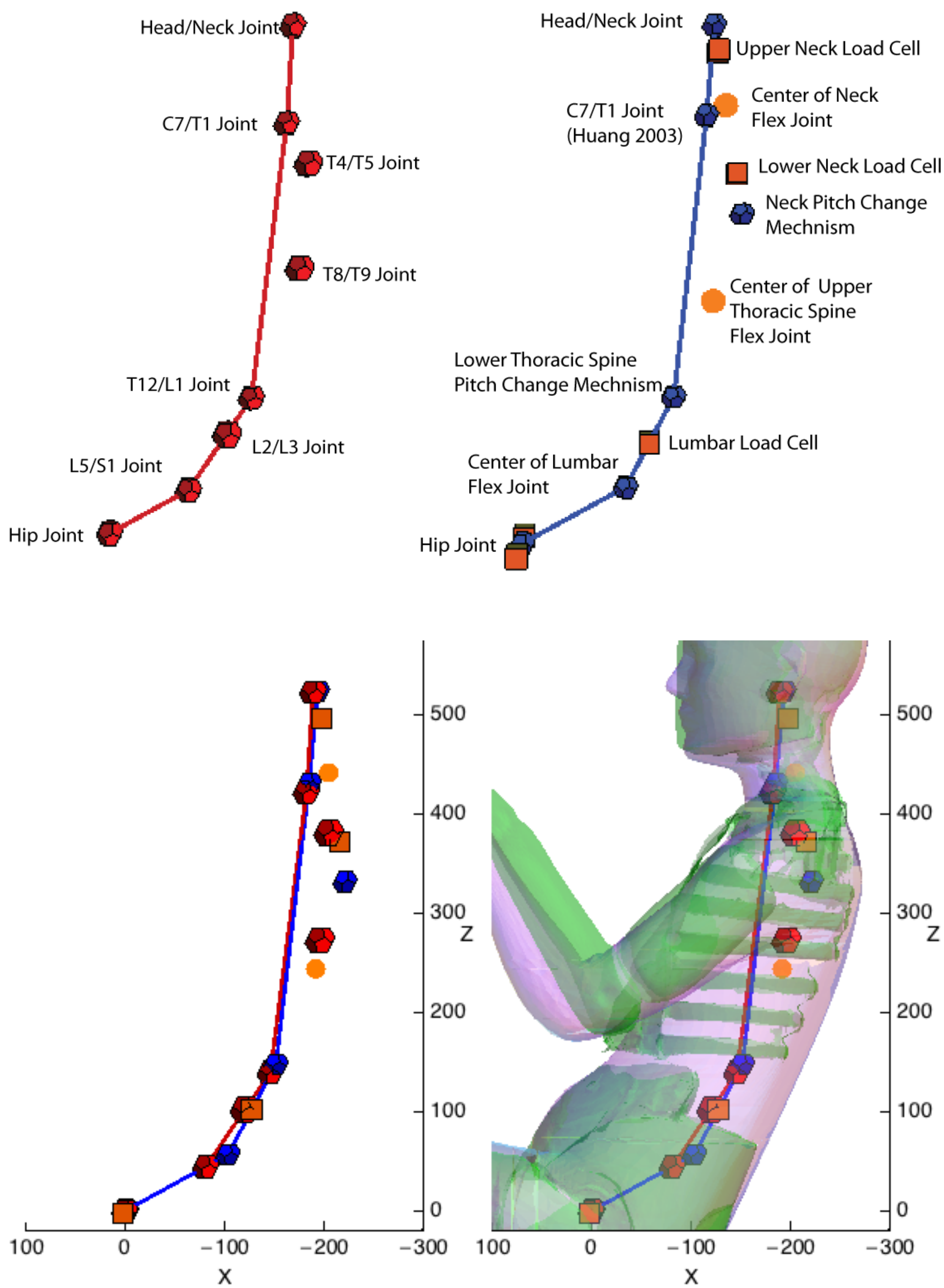

Figure 14. Comparison of skeletal linkage and segment CG locations for AMVO (red) and THOR-05F (blue, green) after articulating limbs and rotating torso segments to align joints.

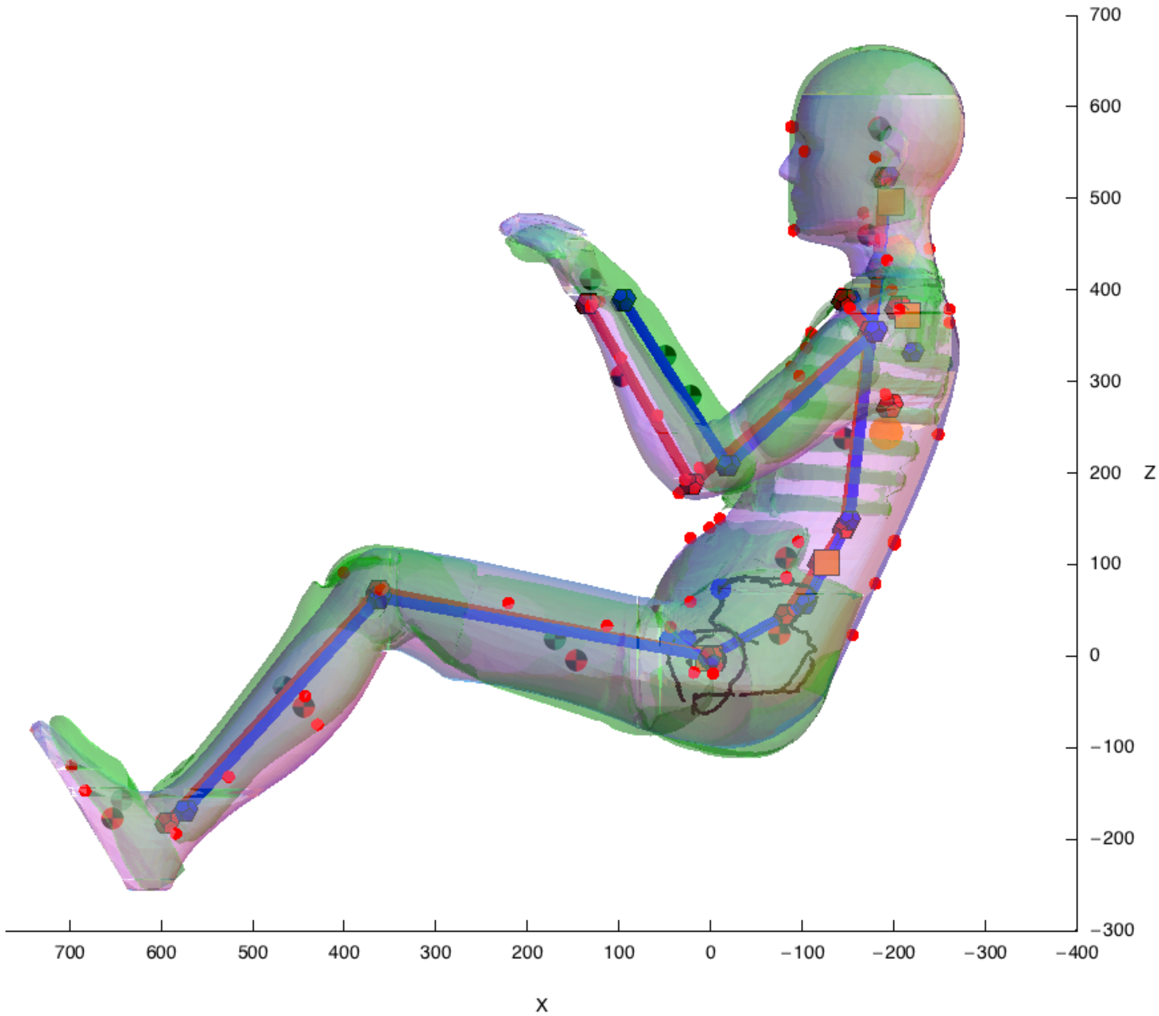

Figure 15. THOR-5F, linkages (blue), CG (green targets) load cells (orange squares) and flex joints (orange circles) aligned to AMVO (linkages red, CG red targets).

Head Angle

Figure 16 shows the scanned head with the measured locations of the O.C. instrument plane, C.G. and estimates of the unmarked glabella and gnathion. In Figure 17 this scan is scaled and laid over a drawing of the THOR-05F design from the GESAC report, aligning on O.C. and the instrumentation shelf. Figure 18 contains the figure from the GESAC report that illustrated the design process used for the THOR-05F head in which the HIII head was aligned to the AMVO head at the O.C. joint and then rotated 2.5 degrees down. The figure also shows the scanned head aligned on the OC with the head rotated so that the instrument shelf is 2.5 degrees down from level.   Figure 19 shows the resulting head locations when the instrument shelf is level (common in positioning procedures), rotated down 2.5 degrees (GESAC report) or up 3.9 degrees to set the instrument shelf to the Frankfort plane angle in AMVO.

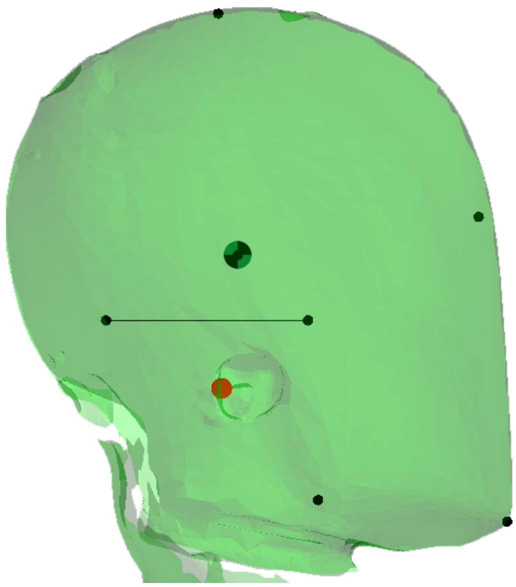

Figure 16. Scanned head with digitized O.C. (red), CG (target) and instrument shelf (line) measured

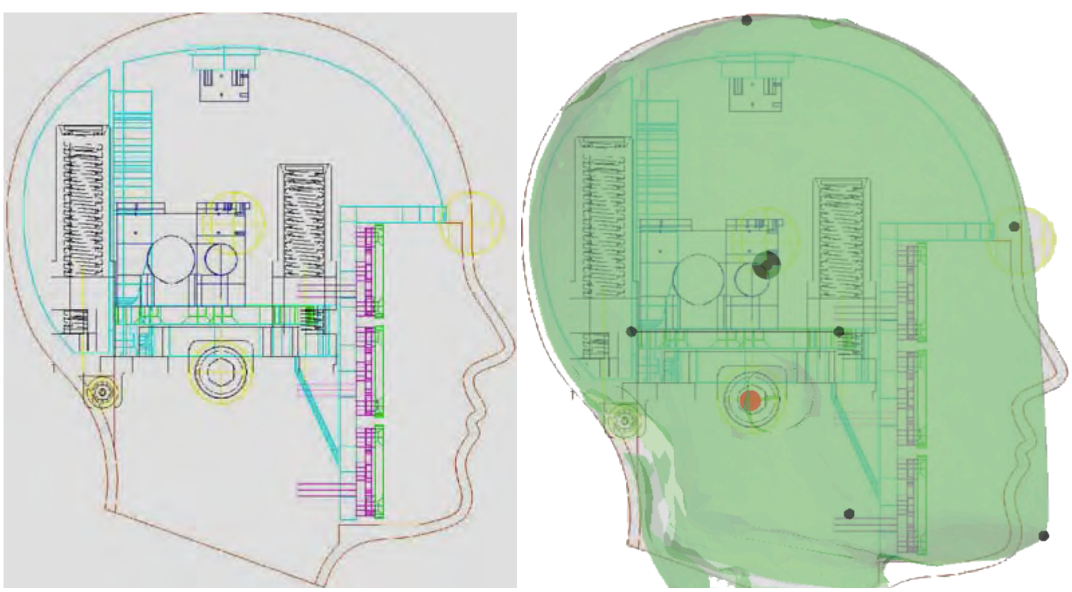

Figure 17. Drawing from GESAC report showing the THOR-5F design head assembly without (left) and with (right) digitized head overlaid and visually scaled using O.C. and top of head and rotated to align to instrument shelf

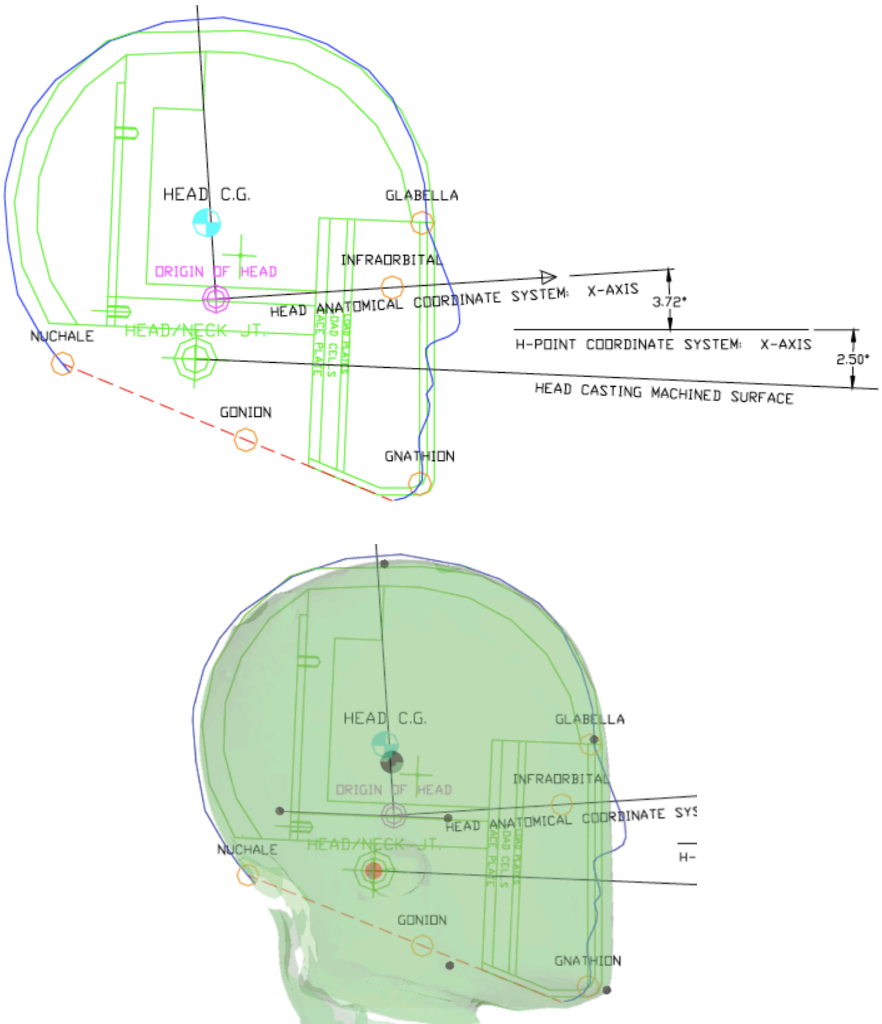

Figure 18. Drawing from GESAC report showing the HIII 5th percentile head on the AMVO 5th female head with landmark design head assembly without (top) and with (bottom) digitized head overlaid, rotated 2.5 degrees down and visually scaled using OC and top of head.

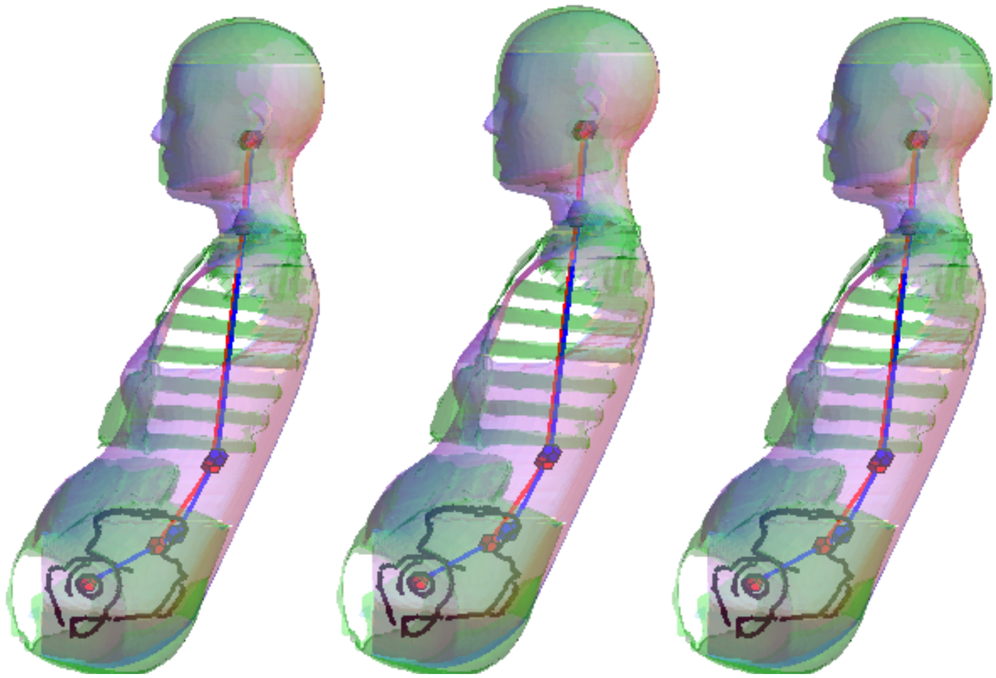

Figure 19. Head instrument plate level (left), head rotated down 2.5 degrees to match GESAC report (middle) or up 3.9 degrees to match AMVO angle (right)

Jacket

The jacket is constructed with heavily treated canvas that is lined with neoprene at the front and back of the chest. Figure 20 shows several 3D views of the jacket isolated from scan data obtained with the jacket on the ATD. Figure 21 shows the jacket laid flat after removal from the ATD. Zipper closures are located along the lateral margins of the thighs and torso and at the tops of the shoulders. This system provides easier and faster access to ATD components during ATD installation than is typically the case with ATD jackets.

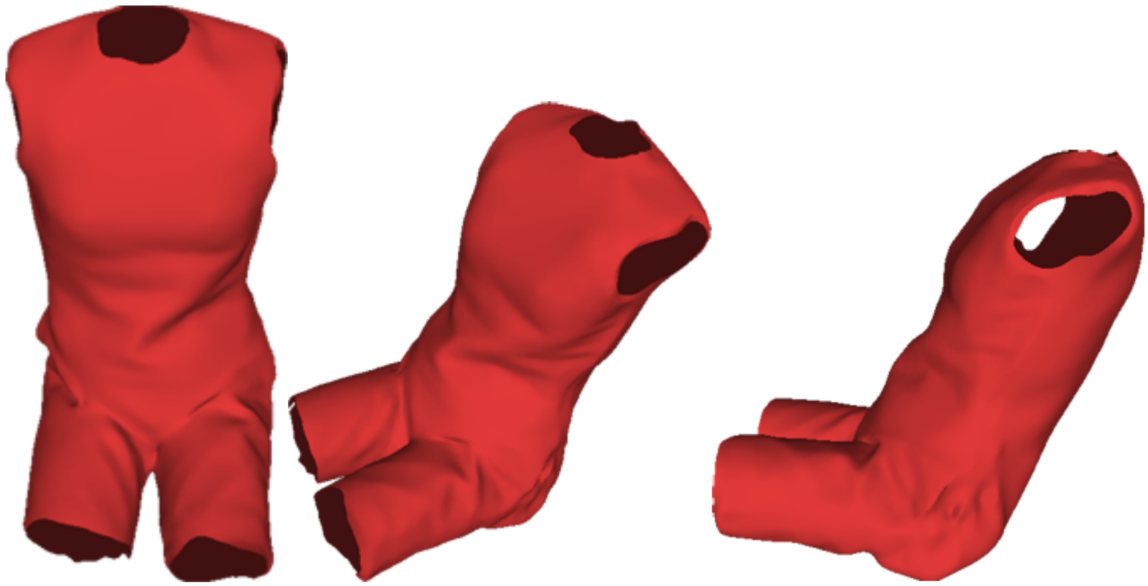

Figure 20. Jacket on ATD (3D scan data).

Figure 21. Jacket removed from ATD and laid flat. Front portion including pockets for breast inserts is at left.

Triangle-shaped, elastic fabric inserts are located along the lateral margins of the abdomen-thigh junctions. Two soft and pliable foam panels on the back and two firmer panels in the front sit behind foam breast inserts. A vinyl backed rubber trapezoid is located over the sternum, presumably to tune chest response. The jacket has a large number of seams to tailor it to the seated ATD shape.

Figure 22 shows detail of the insertion of the two pairs of foam components in the breast area. A rounded "pectoral" foam piece runs approximately superior-inferior in a pocket of fabric. A flat, approximately circularly "breast" piece is placed in a fabric pocket in front of the pectoral piece. Figure 23 shows two alternative locations for the breast pieces that are possible due to extra space in the pockets.

Figure 24 shows a sequence of images from the process of installing the jacket on the ATD. The neck area fits snugly, which may help to control variability in installation in the chest area.

Figure 22. Inserting the pectoral (top) and breast (bottom) forms.

Figure 23. Range of possible positions of "nipple" on breast form due to large pockets (yellow markers).

Figure 24. Installing the jacket (ATD upper extremities removed).

DISCUSSION

Methods

Some of the attributes of the ATD, such as extremity segment masses and CG locations relative to proximal and distal joint locations, could be evaluated relative to the AMVO targets in a relatively straightforward manner. However, most of the other comparisons are considerably more difficult, in part because the ATD was not developed with this type of verification in mind. Specifically, the ATD lacks homologous landmarks that are intended to be representative of corresponding anatomical locations. Consequently, considerable effort was needed to establish meaningful correspondence. Posture differences also confound local geometric differences, creating challenges for comparing overall size and shape. We used a variety of techniques to manipulate 3D geometry after scanning to facilitate the comparison. Finally, important parts of the torso contour are produced by the flexible and compressible jacket, breast, and abdomen components. Experimentation demonstrated the potential for shape variability with repeated installation of these components, which limits the precision of the comparison with the rigid AMVO contour.

Discrepancies and Opportunities for Improvement

Upper Arm Length and Shoulder Posture – The upper arm is approximately 39 mm shorter than the AMVO target. Because the upper extremities are composed of Hybrid-III small-female segments, the discrepancy does not represent a design choice for the THOR-05F. The shoulder posture also differs markedly from the driving posture in the AMVO target. Although it is reasonable that the ATD shoulder be capable of producing both a relaxed, passenger-type posture and a more-forward driving posture, the latter was not readily created with the ATD. The result is a shoulder that may interact differently with the belt than would the shoulder of similar-size human driver. The SD-3 modification of the THOR-50M shoulder includes a new upper arm segment. An adaptation of the SD-3 shoulder to the THOR-05F could include an appropriately scaled upper arm segment.

Buttock and Thigh Contour – The THOR-05F contour differs markedly from the AMVO shell in the buttock and lateral thigh areas. The small-female occupant has exclusively soft tissue, and primarily adipose tissue, in these areas. This tissue is incompressible but relatively mobile, so the human contour is affected by the seat surface interaction. The AMVO contour is intended to approximate the human surface shape when seated in a deformable automobile seat.

The THOR-05F ATD is approximately 65 mm narrower at the hips than the AMVO contour, with the discrepancy extending into the lateral thigh area. The buttock contour of the ATD is also “squarer”, extending laterally at the seat contact surface more than the AMVO contour.

The literature on the design of the THOR-05F does not address the buttock contour. Historically, ATD buttock contours have been squarer than human contours to improve lateral stability when positioning the ATD. ATD flesh also differs from human tissue in being compressible and much less mobile with respect to the skeleton. Due to the lack of mobility, ATD flesh in the buttock and thigh area is generally much stiffer in initial deformation than human tissue. These flesh differences motivate the use of narrower contours for ATDs. A stiff contour as wide as the softer human contour could react unrealistically with seats, although we are not aware of research that has quantified this potential problem.

The consequences of this discrepancy are unclear. One concern is that the narrow ATD might penetrate farther into vehicle seats than similar-size women, resulting in unrealistic belt fit. However, the broader, flatter contour at the seat surface might mitigate this effect.

Spine Linkage – Due to the challenges of positioning neck hardware and instrumentation, the lower neck pivot is substantially lower than the base of the human cervical spine. The longer-than-realistic neck design may provide improved kinematics in impacts, but it may create challenges in matching realistic human posture that deviate substantially from the design posture. However, this is unlikely to be an important problem in practice because of the narrow range of neck postures that will be used with a seated ATD.

Jacket – The unusual jacket construct provides good access to the ATD components during installation. The primary concern is that the positioning of the jacket relative to the underlying components is not well controlled. In particular, the foam components used to represent breast tissue may not be installed consistently in the jacket, and the jacket may not be consistently positioned with respect to the chest and shoulder components, leading to differences in belt placement and thoracic response.

Head – The history of the head development is complex and unclear in many particulars. The central problem is that the available human head anatomy is reported relative to landmarks that do not exist on the ATD. Many of the most important are flesh surface landmarks (tragion, infraorbitale). Lacking these landmarks, the history of the head design shows that the face anatomy of AMVO, which was not intended to be quantitatively representative, has been used as input to the THOR head development process. An improved head could be designed using appropriate landmarks to ensure that the head anthropometry can be verified, the head instrumentation positions and orientations can be accurately interpreted with respect to human occupants, and the head can be representatively positioned for testing.

CONCLUSIONS

1. The THOR-05F, which was designed with reference to the AMVO small-female anthropometry specification, has an overall size and shape that closely matches the AMVO specification.

2. Segment lengths and masses are close to the AMVO specification, except that the upper-arm segment is shorter than the AMVO specification.

3. The shoulder cannot readily be placed into the driving posture represented by the AMVO contour, which might affect the realism of seat belt fit in some circumstances.

4. The THOR-05F buttock contour differs substantially from the AMVO contour, but the differences may represent an appropriate compromise given the differences between ATD and human flesh.

5. The jacket components representing breast tissue may not have sufficient positional control, potentially affecting belt routing and thoracic response.

RECOMMENDATIONS

1. Consideration should be given to lengthening the upper arm segment by 35 mm to better match the AMVO specification.

2. The static positioning of the shoulder components should be examined to determine if a more realistic driving posture can be created.

3. The vertical position of the ATD as installed in vehicle seats should be compared to the positioning of similar-size occupants to address the buttock contour concerns.

4. The effects of the jacket and breast components on belt routing relative to the pelvis, thorax, and shoulder should be examined to determine if greater control of the installation and positioning of these soft components is needed to ensure test repeatability and reproducibility.

5. Future ATD development efforts should include the provision of physical landmarks on the ATD to support anthropometric verification.

REFERENCES

Ebert-Hamilton, S.M. and Reed, M.P. (2011). Evaluation of Hybrid-III 6YO Chest Jacket Shape and Position. Technical Report 2011-1. University of Michigan Transportation Research Institute, Ann Arbor, MI.

GESAC (2005). Development of a Fifth Percentile Female THOR, Task 2 Final Report No: GESAC-05-12, April 2005

Huang, T. J., Shams, T., Rangarajan, N., Haffner, M., Eppinger, R. (2003). Development of an advanced 50th percentile male head/neck system for application to crash test dummies Proceedings of the 18th International Technical Conference on the Enhanced Safety of Vehicles (ESV).

McDonald, J.P., Shams, T., Rangarajan, N., Beach, D., Huang, J-T., Freemire, J., Artis, M., Wang, Y., and Haffner, M. (2003). Design and development of a THOR-based small female crash test dummy. *Stapp Car Crash Journal*, 47:551-570.

Loyd, A. Myers,B. Yoganandan, N., Pintar, F., Ono, K., Marin, P. Nightingale, R. (2007) Recommendations for Inertial and Geometric Properties for the THOR Head, Report to the SAE THOR Evaluation Task Group.

Reed, M.P., and Rupp, J.D. (2013). An anthropometric comparison of current ATDs with the U.S. adult population. *Traffic Injury Prevention.*

Reynolds, H., Snow, C., and Young, J. (1981) Spatial geometry of the human pelvis. Report No. FAA-AM-82-9. Office of Aviation Medicine, Federal Aviation Administration.

Robbins, D.H. (1983) Anthropometric specifications for small female and large male dummies, Volume 3. UMTRI-83-53-3. Final report DOT-HS-806-715. U.S. Department of Transportation, National Highway Traffic Safety Administration, Washington, DC.

Schneider, L.W., Robbins, D.H., Pflüg, M.A., and Snyder, R.G. (1983). Anthropometry of Motor Vehicle Occupants: Development of anthropometrically based design specifications for an advanced adult anthropomorphic dummy family, Volume 1. Final report DOT-HS-806-715. U.S. Department of Transportation, National Highway Traffic Safety Administration, Washington, DC.

Shams, T., Huang, T.J., Rangarajan, N., and Haffner, M. (2003). Design requirements for a fifth-percentile female version of the THOR ATD. Proc. 18th ESV, NHTSA, Washington, DC.

Tylko S, Charlebois D, Bussières A, and Dalmotas D. (2006). The effect of breast anthropometry on the Hybrid III 5th female chest response. *Stapp Car Crash Journal*, 50:389-414.